International Journal of Approximate Reasoning 55 (2014) 1129–1146

Contents lists available at ScienceDirect

International Journal of Approximate Reasoning

www.elsevier.com/locate/ijar

Decomposition of conflict as a distribution on hypotheses in the framework on belief functions

Arnaud Roquel [a], Sylvie Le Hégarat-Mascle [a,*], Isabelle Bloch [b], Bastien Vincke [a]

[a] Institut d'Electronique Fondamentale, Univ. Paris-Sud/CNRS, 91405 Orsay, France
[b] Institut Mines-Telecom, Telecom ParisTech, CNRS LTCI, Paris, France

ARTICLE INFO

Article history:
Received 13 June 2013
Received in revised form 22 December 2013
Accepted 23 December 2013
Available online 31 December 2013

Keywords:
Belief functions
Conflict
Conflict decomposition
Distribution of conflict over hypotheses
Vehicle localization

ABSTRACT

In this paper, we address the problem of identifying the potential sources of conflict between information sources in the framework of belief function theory. To this aim, we propose a decomposition of the global measure of conflict as a function defined over the power set of the discernment frame. This decomposition, which associates a part of the conflict to some hypotheses, allows identifying the origin of conflict, which is hence considered as "local" to some hypotheses. This is more informative than usual global measures of conflict or disagreement between sources. Having shown the unicity of this decomposition, we illustrate its use on two examples. The first one is a toy example where the fact that conflict is mainly brought by one hypothesis allows identifying its origin. The second example is a real application, namely robot localization, where we show that focusing the conflict measure on the "favored" hypothesis (the one that would be decided) helps us to robustify the fusion process.

1. Introduction

Multi-sensor systems are used in many applications such as classification, image processing, change detection, object trajectory localization. Usually the information provided by each sensor is prone to imperfections, such as imprecision and uncertainty, and fusion procedures aim at making better decisions by combining multi-sensor information. Belief Functions (BF) are suitable for modeling imprecision and uncertainty, and handle belief on the power set of the frame of discernment (set of hypotheses).

A disagreement between sources indicates a possibly unreliable result from which may derive a bad decision. Thus, for managing the disagreement, several authors have developed different combination rules where "Dempster's conflict" [48] is transferred to a set of elements. There are two main ways to redistribute Dempster's conflict: Either globally, using Dempster's rule [45] or Yager's rule [52], or based on a conflict estimation local to a considered hypothesis, for instance using Dubois and Prade's rule [12], which can be considered as a redistribution rule (although not initially intended as such), as shown in [21], or using a Proportional Conflict Redistribution rule (e.g. PCR5 [47]). In [25,28], the conflict is estimated locally to a hypothesis and a source, and relatively to the other hypotheses supported by the other sources. This local estimation is assumed to be a local indicator of source "reliability", and then used to automatically discount the source. Florea et al. [14] proposed a more robust (according to the authors) combination that is a weighted sum of conjunctive and disjunctive rules, with the weights being functions of Dempster's conflict.

A few works have proposed to use the conflict in other tasks than the one of combination. For instance, in [37,38], Dempster's conflict was used as a precision criterion of superimposition of the images provided by the different sources. The authors in [35] proposed to use the conflict between a model predicting the evolution of a system state and observations

* Corresponding author.

0888-613X/$ – see front matter
http://dx.doi.org/10.1016/j.ijar.2013.12.006

to decide whether the model was appropriate or not, and then potentially change the model. Schubert [41,42] proposed to compute pairwise conflicts between sources, to use the conflict values for clustering the sources, and to combine only non-conflicting sources (grouped into the same cluster). In the same spirit, Klein and Colot [19] defined a series of measures of conflict that is function of discounting rates and based singular source mining on it. In [43], a measure involving both Dempster's conflict and the aggregated uncertainty [24,16,29,17] was used to evaluate the relevance of different discernment frames.

Finally, besides these studies considering the conflict as a potential information source, several works focused on the estimation of the conflict itself. A review can be found in [22], where the author argues that two beliefs in conflict should present both a high Dempster's conflict value and a high distance value. Indeed, the dissimilarity between beliefs is often measured by a distance (see [18] for a review of the different distance measures between beliefs). A typical example is to compute an L_p-norm distance between mass functions. In [27], Jousselme's distance was used to evaluate the conflict introduced by a belief into a set of beliefs. Now, authors generally agree that a distance is not a direct measure of conflict. Recently, some works have proposed alternative definitions to Dempster's conflict, e.g. [9,26,43,44,11]. Anyway, Dempster's conflict remains a strong indicator, even if its interpretation may not be so straightforward.

In this paper, that extends our preliminary work in [40], we aim at a finer analysis of source disagreement based on Dempster's conflict. In particular, we propose a decomposition of Dempster's conflict, which is related to the different elements of the frame of discernment and thus helps identifying the potential link between the conflict and particular hypotheses. It only applies for non-dogmatic belief.

The proposed decomposition can be used to analyze the intra-source conflict (i.e. the conflict inherent to a source when modeling the information it delivers as belief functions) or the conflict between sources (i.e. the conflict which appears when merging sources). This decomposition could also be used to design new combination rules. This step is out of the scope of this paper and we focus on the decomposition and its analysis.

After reminding some notations and basic elements on mass function decompositions and distance measures in Section 2, the proposed function of conflict is introduced and analyzed in Section 3, while numerical aspects are detailed in Section 4. It is then illustrated on a vehicle localization problem in Section 5. Conclusions are provided in Section 6.

2. Background

In the following, we denote by Ω the frame of discernment and by 2^Ω the power set of Ω. A Basic Belief Assignment (BBA) on 2^Ω, noted m and also called mass function, is a function from 2^Ω into $[0,1]$ such that $\sum_{A\in 2^\Omega} m(A) = 1$. The elements A of 2^Ω with a non-null mass value, i.e. $m(A) > 0$, are called the focal elements of the BBA. Three specific kinds of BBAs are:

- the BBAs, called "non-dogmatic", that have Ω as focal element,
- the BBAs having only two focal elements, one of which being Ω, called "Simple Support Functions (SSF)" when referring to the canonical decomposition (presented further),
- the BBAs, called "consonant", that have nested focal elements, i.e. $\forall A \subseteq \Omega \mid m(A) > 0$, $\forall B \subseteq \Omega \mid m(B) > 0$, $A \subseteq B$ or $B \subseteq A$.

Plausibility and commonality are denoted by Pl and q, respectively. They are functions on 2^Ω: $\forall A \in 2^\Omega$, $Pl(A) = \sum_{B\cap A\neq\emptyset} m(B)$, $q(A) = \sum_{B\supseteq A} m(B)$. Note that since the functions m, Pl and q (as the two other belief functions not used in this work, namely the credibility Bel and the implicability b) are in one to one correspondence, they represent the same belief.

The dissimilarity between BBAs is often used for computing the disagreement between the corresponding sources. As said in the Introduction, it is generally estimated from a conflict or distance measure (see e.g. [18,22]). Specifically, "Dempster's conflict" is computed, in the case of two BBAs m_1 and m_2, as follows:

$$K_{1,2} = \sum_{A\subseteq\Omega} \sum_{\substack{B\subseteq\Omega \\ A\cap B=\emptyset}} m_1(A)m_2(B). \tag{1}$$

When several beliefs are available, combining them allows deriving a global belief. Specifically, the orthogonal sum was defined by Dempster [45] to combine, in a conjunctive way, N BBAs assumed to be independent. It involves a normalization term that corresponds to the assumption of a closed world[1] and writes, in the case of two BBAs m_1 and m_2, $1 - K_{1,2}$ (Eq. (1)). Alternatively, assuming an open world,[2] Smets proposed [49] to remove the normalization and to assign the value $K_{1,2}$ to the mass of the empty set. Then, Smets' combination [49] (sometimes simply called conjunctive rule because of its authority) writes:

[1] Exhaustive discernment frame.
[2] Non-exhaustive discernment frame.

$$\forall C \subseteq \Omega, \quad m_{1 \textcircled{\cap} 2}(C) = \sum_{A \subseteq \Omega} \sum_{\substack{B \subseteq \Omega \\ A \cap B = C}} m_1(A) m_2(B). \tag{2}$$

The dual operator to the combination is the decomposition. It aims at deriving the elementary beliefs underlying a global belief. In the canonical decomposition initially proposed by Shafer [45], the elementary beliefs were SSFs, and when a BBA can be represented as an orthogonal sum of SSFs, it is said "separable" (SBBA). Then, Smets proposed a canonical decomposition of every non-dogmatic BBA, as a unique conjunctive combination of generalized simple support functions (GSSF) [49]:

$$m = \bigcirc_{A \subset \Omega} A^{w(A)}, \tag{3}$$

where $A^{w(A)}$ is a GSSF, i.e. a function with only two focal elements A and Ω, such that $A^{w(A)}(\Omega) = w(A)$, $A^{w(A)}(A) = 1 - w(A)$, and $\forall B \in 2^{\Omega} \setminus \{A, \Omega\}$, $A^{w(A)}(B) = 0$. If $w(A) \leqslant 1$ then $A^{w(A)}$ is an SSF, and if all the GSSFs of the canonical decomposition are SSFs, m in Eq. (3) is an SBBA.

By convention Ω is not part of the canonical decomposition, and we set $w(\Omega) = 1$ in the following. For the other elements of the decomposition, the weight function w is expressed from the commonalities:

$$\forall A \subset \Omega, \quad w(A) = \prod_{B \supseteq A} q(B)^{(-1)^{|B|-|A|+1}}. \tag{4}$$

The canonical decomposition has been used, for instance, to define a cautious combination rule taking into account the non-independence between sources: the decomposition helps to recognize similar elementary beliefs that are present in both BBAs to combine. Then, for the conjunctive combination of N non-dogmatic BBAs that are not "cognitively independent", Denoeux' cautious rule [10] writes: $m_{\textcircled{\wedge}} = \bigcirc_{A \subset \Omega} A^{\bigwedge_{j=1}^{N} w_j(A)}$, where $\bigwedge$ usually denotes the minimum operator. Using the canonical decomposition, Smets' combination can be reexpressed in the case of N non-dogmatic BBAs that are "cognitively independent":

$$\forall A \subset \Omega, \quad m_{\textcircled{\cap}}(A) = \bigcirc_{A \subset \Omega} A^{\prod_{j=1}^{N} w_j(A)}. \tag{5}$$

In our case, we will mainly use the canonical decomposition to recover the elementary beliefs.

Finally, the pignistic probability function *BetP* is widely used at decision level within the Transferable Belief Model interpretation of belief functions [48]. It is defined from Ω into $[0, 1]$ such that $\forall H \in \Omega$, $BetP(H) = \frac{1}{m(\emptyset)} \sum_{A \in 2^{\Omega}, H \in A} \frac{m(A)}{|A|}$, where $|A|$ denotes the cardinality of A.

In the following, according to the previous notations, H denotes a singleton hypothesis, and A any subset of Ω.

3. Proposed decomposition of conflict

In this study, we aim at developing a more informative measure of the conflict than a single scalar value. In particular, it seems important to determine the different contributions of the hypotheses to the global conflict between sources. For instance it could help to detect a modeling problem specific to a given hypothesis (as shown in Section 4.3) or to evaluate the consensual nature of a hypothesis likely to be decided (as shown in Section 5). This is achieved by a decomposition of $m(\emptyset)$ that leads to the definition of a function of conflict defined over the power set of the discernment frame.

In this study we assume that $m(\emptyset)$ is given. It could either have appeared after the combination of two (or more) BBAs using an unnormalized combination rule, or have been present in the initial BBA(s), for instance, when modeling a reject hypothesis under an open-world assumption. Now, in the considered application and in the toy example cited for the illustration of the proposed decomposition interpretation, only the first case has been considered since the second one is very specific. Anyway, all the developments in this section apply whatever the origin of $m(\emptyset)$.

3.1. Functions $f_{\emptyset}$ and $\overline{f_{\emptyset}}$

Let m be a non-dogmatic BBA. We denote by $\mathcal{C}$ the subset of 2^{Ω} such that $\mathcal{C} = \{A \in 2^{\Omega} \mid w(A) \neq 1\}$, where w is the weight function of m. Note that $\Omega \notin \mathcal{C}$.

Definition 1 *(Conflicting subsets $\Gamma_{\emptyset_l}$).* Let m be a non-dogmatic BBA and the associated $\mathcal{C}$. We define a conflicting subset of cardinality p as a subset $\Gamma_{\emptyset_l} = \{A_1, \ldots, A_p\}$ of $\mathcal{C}$, such that $\bigcap_{i=1}^{p} A_i = \emptyset$ and $\nexists (A_i, A_j) \in \Gamma_{\emptyset_l}^2, i \neq j \mid A_i \subseteq A_j$.

Definition 2 *(Set of conflicting subsets $\mathcal{S}_{\Gamma}$).* The set $\mathcal{S}_{\Gamma}$ is the set of all subsets $\Gamma_{\emptyset_l}$. It is a finite set, we note L its cardinality.

For instance, for $\Omega = \{H_1, H_2, H_3\}$, $\{H_1, \{H_1, H_2\}, \{H_2, H_3\}, \{H_1, H_3\}\}$ is not an element of $\mathcal{S}_{\Gamma}$, while the reduced subsets $\{H_1, \{H_2, H_3\}\}$ and $\{\{H_1, H_2\}, \{H_2, H_3\}, \{H_1, H_3\}\}$ are.

Definition 3 *(Function $f_\emptyset$).* Let $\mathcal{S}_\Gamma = \{\Gamma_{\emptyset_l},\ l \in \{1,\dots L\}\}$ as in Definition 2. We define a function $f_\emptyset$ from $\mathcal{S}_\Gamma$ into $\mathbb{R}$ as:

$$\forall \Gamma_{\emptyset_l} \in \mathcal{S}_\Gamma, \quad f_\emptyset(\Gamma_{\emptyset_l}) = \prod_{A_i \in \Gamma_{\emptyset_l}} \big(1 - w(A_i)\big) \prod_{\substack{A_k \in \mathcal{C} | \\ \forall A_j \in \Gamma_{\emptyset_l},\ A_j \cap A_k \neq A_j}} w(A_k). \tag{6}$$

In Eq. (6), the first part of $f_\emptyset(\Gamma_{\emptyset_l})$, namely $\prod_{A_i \in \Gamma_{\emptyset_l}} (1 - w(A_i))$, represents the conflict directly induced by the elements of $\Gamma_{\emptyset_l}$ (the term "direct conflict" was introduced in [45] to qualify the conflict between two SSFs). The second part of $f_\emptyset(\Gamma_{\emptyset_l})$, namely $\prod_{\substack{A_k \in \mathcal{C} | \forall A_j \in \Gamma_{\emptyset_l}, \\ A_j \cap A_k \neq A_j}} w(A_k)$, represents a discounting of the previous direct conflict (case of an SBBA).

Proposition 1. *The function $f_\emptyset$ introduced in Definition 3 can be expressed as*:

$$\forall \Gamma_{\emptyset_l} \in \mathcal{S}_\Gamma, \quad f_\emptyset(\Gamma_{\emptyset_l}) = \prod_{A_i \in \Gamma_{\emptyset_l}} A_i^{w(A_i)}(A_i) \prod_{A_j \notin \Gamma_{\emptyset_l}} \sum_{\substack{B \in \{A_j, \Omega\} | \\ \exists A_i \in \Gamma_{\emptyset_l},\ A_i \subsetneq B}} A_j^{w(A_j)}(B). \tag{7}$$

Proof. By definition, $\forall A_i \in \Gamma_{\emptyset_l}$,

$$A_i^{w(A_i)}(A_i) = 1 - w(A_i). \tag{8}$$

Then, $\forall A_j \notin \Gamma_{\emptyset_l}$,

$$\sum_{\substack{B \in \{A_j, \Omega\} | \\ \exists A_i \in \Gamma_{\emptyset_l},\ A_i \subsetneq B}} A_j^{w(A_j)}(B) = \begin{cases} w(A_j) & \text{if } \nexists A_i \in \Gamma_{\emptyset_l} \mid A_i \subsetneq A_j, \\ 1 & \text{if } \exists A_i \in \Gamma_{\emptyset_l} \mid A_i \subsetneq A_j. \end{cases} \tag{9}$$

Then,

$$\prod_{A_j \notin \Gamma_{\emptyset_l}} \sum_{\substack{B \in \{A_j, \Omega\} | \\ \exists A_i \in \Gamma_{\emptyset_l},\ A_i \subsetneq B}} A_j^{w(A_j)}(B) = \prod_{\substack{A_j \notin \Gamma_{\emptyset_l} | \\ \forall A_i \in \Gamma_{\emptyset_l},\ A_i \cap A_j \neq A_i}} w(A_j) \tag{10}$$

$$= \prod_{\substack{A_k \in \mathcal{C} | \\ \forall A_i \in \Gamma_{\emptyset_l},\ A_i \cap A_k \neq A_i}} w(A_k). \quad \square \tag{11}$$

Definition 4 *(Local conflict function $\overline{f_\emptyset}$).* Using the same notations, we define an average function $\overline{f_\emptyset}$, called "local conflict function", from 2^Ω into $\mathbb{R}$ as:

$$\forall A \subsetneq \Omega, \quad \overline{f_\emptyset}(A) = \sum_{\Gamma_{\emptyset_l} | A \in \Gamma_{\emptyset_l}} \frac{1}{|\Gamma_{\emptyset_l}|} f_\emptyset(\Gamma_{\emptyset_l}),$$

$$\overline{f_\emptyset}(\Omega) = 0. \tag{12}$$

3.2. Proposed decomposition of $m(\emptyset)$

In this section, we illustrate the interest of the previous definitions of $f_\emptyset$ and $\overline{f_\emptyset}$, by showing that $m(\emptyset) = \sum_{A \in 2^\Omega} \overline{f_\emptyset}(A)$. For this, let us first decompose $m(\emptyset)$ over the $f_\emptyset(\Gamma_{\emptyset_l})$ for $\Gamma_{\emptyset_l} \in \mathcal{S}_\Gamma$.

Proposition 2. *Let m be a non-dogmatic BBA, $\mathcal{S}_\Gamma = \{\Gamma_{\emptyset_l},\ l \in \{1 \dots L\}\}$ as in Definition 2 and $f_\emptyset$ as in Definition 3. The mass on the empty set can be expressed as*:

$$m(\emptyset) = \sum_{\Gamma_{\emptyset_l} \in \mathcal{S}_\Gamma} f_\emptyset(\Gamma_{\emptyset_l}). \tag{13}$$

Proof. m is the conjunction of the GSSFs of the canonical decomposition, and in particular $m(\emptyset)$ writes:

$$m(\emptyset) = \sum_{\substack{B_i \subseteq \Omega, i \in \{1,\dots,|\mathcal{C}|\} | \\ B_1 \cap B_2 \cap \dots \cap B_{|\mathcal{C}|} = \emptyset}} A_1^{w(A_1)}(B_1) \times \dots \times A_{|\mathcal{C}|}^{w(A_{|\mathcal{C}|})}(B_{|\mathcal{C}|}). \tag{14}$$

Now, $\forall i \in \{1 \dots |\mathcal{C}|\}$, $A_i^{w(A_i)}$ is a GSSF whose mass value is null except for $B_i \in \{A_i, \Omega\}$. Therefore,

$$m(\emptyset) = \sum_{B_1 \in \{A_1, \Omega\}} \cdots \sum_{\substack{B_{|\mathcal{C}|} \in \{A_{|\mathcal{C}|}, \Omega\}| \\ \bigcap_{i=1}^{|\mathcal{C}|} B_i = \emptyset}} \prod_{i=1}^{|\mathcal{C}|} A_i^{w(A_i)}(B_i). \tag{15}$$

Let S_B denote a set of $|\mathcal{C}|$ elements where each element B_i is chosen between A_i and Ω: $S_B = \{B_i \in \{A_i, \Omega\},\ i \in \{1, \dots, |\mathcal{C}|\} \mid \bigcap_{i=1}^{|\mathcal{C}|} B_i = \emptyset\}$. The right member of Eq. (15) is a sum over elements S_B. Now, for any set S_B involved in this sum, two possibilities arise:

- this set does not contain consonant subsets, and then it is an element of $\mathcal{S}_\Gamma$;
- this set contains consonant subsets. Then a subset of it is an element of $\mathcal{S}_\Gamma$, with cardinality lower than $|\mathcal{C}|$. Let $\Gamma_{\emptyset_l}^{S_B}$ denote the subset of S_B obtained by removing from S_B the B_j of largest cardinalities among the consonant ones. Note that several S_B can lead to the same $\Gamma_{\emptyset_l}^{S_B}$ when using this procedure. Let us consider an element $\Gamma_{\emptyset_l}$ of $\mathcal{S}_\Gamma$, and all sets S_B such that $\Gamma_{\emptyset_l}^{S_B} = \Gamma_{\emptyset_l}$. Then the contribution to $m(\emptyset)$ of all these sets S_B is:

$$\begin{aligned} &\sum_{B_1 \in \{A_1, \Omega\}} \cdots \sum_{\substack{B_{|\mathcal{C}|} \in \{A_{|\mathcal{C}|}, \Omega\}| \\ \{B_i\}_{i \in \{1 \dots |\mathcal{C}|\}} = S_B, \Gamma_{\emptyset_l}^{S_B} = \Gamma_{\emptyset_l}}} \prod_{B_i \in S_B} A_i^{w(A_i)}(B_i) \\ &= \prod_{A_i \in \Gamma_{\emptyset_l}} A_i^{w(A_i)}(A_i) \times \prod_{A_j \notin \Gamma_{\emptyset_l}} \sum_{\substack{B \in \{A_j, \Omega\}| \\ \exists A_i \in \Gamma_{\emptyset_l},\ A_i \subsetneq B}} A_j^{w(A_j)}(B) = f_\emptyset(\Gamma_{\emptyset_l}). \end{aligned} \tag{16}$$

Reciprocally, for each $\Gamma_{\emptyset_l} \in \mathcal{S}_\Gamma$, each way to supplement it by $|\mathcal{C}| - |\Gamma_{\emptyset_l}|$ elements $B \in \mathcal{C} \cup \Omega$ such that $\exists A_i \in \Gamma_{\emptyset_l}$, $A_i \subsetneq B$ forms a set $\{B_i \in \{A_i, \Omega\}, i \in \{1, \dots, |\mathcal{C}|\} \mid \bigcap_{i=1}^{|\mathcal{C}|} B_i = \emptyset\}$ and thus is an element involved in the sum of Eq. (15).

Finally we get:

$$m(\emptyset) = \sum_{\Gamma_{\emptyset_l} \in \mathcal{S}_\Gamma} \left(\prod_{A_i \in \Gamma_{\emptyset_l}} A_i^{w(A_i)}(A_i) \times \prod_{A_j \notin \Gamma_{\emptyset_l}} \left[\sum_{\substack{B \in \{A_j, \Omega\}| \\ \exists A_i \in \Gamma_{\emptyset_l}, |A_i \subsetneq B}} A_j^{w(A_j)}(B) \right] \right). \tag{17}$$

From this expression and Eq. (7), Eq. (13) is straightforward. □

For instance, let $\Omega = \{H_1, H_2, H_3, H_4\}$ and $\mathcal{C} = \{H_1, H_2, H_4, \{H_1, H_4\}\}$. The set $S_B = \{H_1, H_2, H_4, \{H_1, H_4\}\}$ is involved in the sum of Eq. (15). Then, the element of $\mathcal{S}_\Gamma$ associated with S_B is in $\{\{H_1, H_2\}, \{H_1, H_4\}, \{H_2, H_4\}, \{H_2, \{H_1, H_4\}\}, \{H_1, H_2, H_4\}\}$. By specifying that this element of $\mathcal{S}_\Gamma$ is supplemented by only hypotheses B such that $\exists A_i \in \Gamma_{\emptyset_l} \mid A_i \subsetneq B$, there is only one associated conflicting subset $\Gamma_{\emptyset_l}^{S_B}$, namely $\{H_1, H_2, H_4\}$. Reciprocally, for $\Gamma_{\emptyset_l} = \{H_1, H_2\}$, there are two associated sets S_B, namely $\{H_1, H_2, \Omega, \{H_1, H_4\}\}$ and $\{H_1, H_2, \Omega, \Omega\}$.

This expression shows that the mass of the empty set is the sum of L "partial conflicts", introduced by subsets of elements in direct conflict (elements present in the conflictual subset $\Gamma_{\emptyset_l}$), and whose value is discounted by some not conflicting terms.

The next proposition is the main result of the paper, namely the interpretation of $\overline{f_\emptyset}$ as a decomposition of the mass of the empty set.

Proposition 3. *Using the same notations as above, we have*:

$$m(\emptyset) = \sum_{A \in 2^\Omega} \overline{f_\emptyset}(A). \tag{18}$$

Proof. We have:

$$\sum_{A \in 2^\Omega} \overline{f_\emptyset}(A) = \sum_{A \in 2^\Omega} \left[\sum_{\Gamma_{\emptyset_l} | A \in \Gamma_{\emptyset_l}} \frac{1}{|\Gamma_{\emptyset_l}|} f_\emptyset(\Gamma_{\emptyset_l}) \right] = \sum_{l=1}^{L} \frac{1}{|\Gamma_{\emptyset_l}|} \sum_{A \in \Gamma_{\emptyset_l}} f_\emptyset(\Gamma_{\emptyset_l}).$$

Now, for a given conflicting subset $\Gamma_{\emptyset_l}$, the sum $\sum_{A \in \Gamma_{\emptyset_l}} f_\emptyset(\Gamma_{\emptyset_l})$ includes $|\Gamma_{\emptyset_l}|$ identical terms ($f_\emptyset(\Gamma_{\emptyset_l})$), since $\Gamma_{\emptyset_l}$ is a set (not ordered). Then, $\sum_{A \in 2^\Omega} \overline{f_\emptyset}(A) = \sum_{l=1}^{L} f_\emptyset(\Gamma_{\emptyset_l}) = m(\emptyset)$. □

The values taken by the function $\overline{f_\emptyset}$ at a point (hypothesis) are the terms of the decomposition. Thus, they may be viewed as the parts of the conflict "local" to a given hypothesis, hence the proposed name "local conflict function" in opposition to Dempster's conflict that is a "global conflict" measure. Let us also recall that the proposed decomposition only applies for a non-dogmatic BBA. Then, considering a non-dogmatic BBA, the canonical decomposition allows us to decompose it in elementary beliefs (or "unbeliefs" in the case of a non-SSBA). These elementary beliefs can be in conflict or not, and the proposed decomposition puts in light the parts of the conflict due to the different subsets of the elements of the canonical decomposition.

Proposition 4. *The decomposition of $m(\emptyset)$ given by Eq. (18) is unique.*

Proof. According to Eq. (6), $f_\emptyset(\Gamma_{\emptyset_l})$ only depends on the canonical decomposition of the considered BBA. From this canonical decomposition, we derive: (i) the set $\mathcal{C}$ and thus the set S_Γ according to Definition 2, and (ii) the weight function w. Thus the function $f_\emptyset$ is unique for a given BBA, and so is the function $\overline{f_\emptyset}$, and the decomposition of $m(\emptyset)$. □

Corollary 1. *For an SBBA, $\forall A \in 2^\Omega$, $\overline{f_\emptyset}(A) \in [0,1]$.*

Proof. Since the BBA is separable, $\forall A \in 2^\Omega$, $w(A) \in (0,1]$. Therefore, according to Eq. (6), $\forall \Gamma_{\emptyset_l} \in \mathcal{S}_\Gamma$, $f_\emptyset(\Gamma_{\emptyset_l}) \in [0,1]$, and according to Eq. (12), $\forall A \in 2^\Omega$, $\overline{f_\emptyset}(A) \geqslant 0$. Thus, from Eq. (18), $m(\emptyset)$ is a sum of positive terms. Besides it is bounded by 1, therefore $\forall A \in 2^\Omega$, $\overline{f_\emptyset}(A) \in [0,1]$. □

Corollary 2. *For a normalized consonant BBA, $\forall A \in 2^\Omega$, $\overline{f_\emptyset}(A) = 0$.*

Proof. Since the BBA is consonant, $\mathcal{C}$ is also consonant ($\mathcal{C}$ is a subset of the focal element set). Then, there is no conflicting subset and $\mathcal{S}_\Gamma = \emptyset$. Thus, $\forall A \in 2^\Omega$, $\overline{f_\emptyset}(A) = 0$. □

4. Numerical aspects

4.1. Example of algorithm

Practically, there are four main steps to compute the conflict decomposition of a BBA m:

1. compute the canonical decomposition of m and its weight function w;
2. compute the set $\mathcal{S}_\Gamma$ of conflicting subsets $\Gamma_{\emptyset_l}$;
3. compute the values of the function $f_\emptyset$ according to Eq. (6);
4. compute the values of the function $\overline{f_\emptyset}$ according to Eq. (12).

One difficulty may be the estimation of $\mathcal{S}_\Gamma$ when $|\mathcal{C}|$ is large. According to Definition 1, the elements $\Gamma_{\emptyset_l}$ of $\mathcal{S}_\Gamma$ are such that $\nexists (A_i, A_j) \in \Gamma_{\emptyset_l} \times \Gamma_{\emptyset_l},\ i \neq j \mid A_i \subseteq A_j$. Let us define $\mathcal{C}^* = \mathcal{C} \setminus \{\emptyset\}$ ($\mathcal{C}^*$ is the restriction of $\mathcal{C}$ to non-null elements), and $\mathcal{C}_0 = \{\emptyset\}$.

In the following definition, we decompose $\mathcal{C}^*$ as a partition into consonant subsets $\mathcal{C}_j$ defined as follows:

Definition 5 *(Subsets $\mathcal{C}_j$).* For a non-dogmatic BBA m and the associated set $\mathcal{C}$, let $\{\mathcal{C}_j,\ j \in \{1,\dots,M\}\}$ be a set of M subsets that form a partition of $\mathcal{C}^*$, and such that each element of the partition is consonant, i.e. $\forall (A,B) \in \mathcal{C}_j^2$, $A \subseteq B$ or $B \subseteq A$.

For instance, let $\Omega = \{H_1, \dots H_6\}$ and $\mathcal{C} = \{A_1, \dots A_6\}$ with $A_1 = \{H_1\}$, $A_2 = \{H_1, H_3\}$, $A_3 = \{H_2\}$, $A_4 = \{H_2, H_4, H_5\}$, $A_5 = \{H_1, H_3, H_4\}$, $A_6 = \{H_2, H_6\}$. An example of partition of $\mathcal{C}$ into $M = 4$ subsets is as follows: $\mathcal{C}_1 = \{A_1, A_2\}$, $\mathcal{C}_2 = \{A_3, A_4\}$, $\mathcal{C}_3 = \{A_5\}$, $\mathcal{C}_4 = \{A_6\}$. An example of partition of $\mathcal{C}$ into $M = 3$ subsets is as follows: $\mathcal{C}_1 = \{A_1, A_2, A_5\}$, $\mathcal{C}_2 = \{A_3, A_6\}$, $\mathcal{C}_3 = \{A_4\}$.

From Definition 1, two elements of $\Gamma_{\emptyset_l}$ cannot belong to the same subset $\mathcal{C}_j$: $\forall (A_i, A_{i'}) \in \Gamma_{\emptyset_l}^2$, $(A_i \in \mathcal{C}_j,\ A_{i'} \in \mathcal{C}_{j'},\ i \neq i') \Rightarrow j \neq j'$. Then $|\Gamma_{\emptyset_l}| \leqslant M$, with M the number of consonant subsets $\mathcal{C}_j$. Then, a simple method to derive $\mathcal{S}_\Gamma$ is provided in Algorithm 1.

An intermediate variable in Algorithm 1 is the indicator vector V. The correspondence between the different p-tuples with $p \in \{0,\dots,M\}$ and the V indices is as follows (in our case): an M-tuple of indices $(i_M, \dots, i_1)$, with $\forall j \in \{1,\dots,M\}$, $i_j \in \{0,\dots,|\mathcal{C}_j|\}$, corresponds to a p-tuple of $\mathcal{C}$ elements such that i_j is the index of the element selected in $\mathcal{C}_j$ with the convention that $i_j = 0$ means that no element is selected in $\mathcal{C}_j$. Then, this M-tuple of indices $(i_M, \dots, i_1)$ is located in V at the position $\sum_{j=1}^{M} i_j s_j$ with $s_1 = 1$ and $\forall j \in \{2,\dots,M\}, s_j = \prod_{k=1}^{j-1}(|\mathcal{C}_k| + 1) = s_{j-1}(|\mathcal{C}_{j-1}| + 1)$. Thus for an element of V located at position n, the index of the $\mathcal{C}_j$ element is $\frac{n}{s_j} \pmod{|\mathcal{C}_j| + 1}$, where $\frac{x}{y}$ is the entire division.

In Algorithm 3, the first step after initialization is the setting to 0 of the components of V corresponding to the M-tuples actually containing less than 2 elements of $\mathcal{C}$ (only 1 or 0 $i_j > 0$ in the M-tuple of indices $(i_M, \dots, i_1)$). Then, the second part

Algorithm 1: Conflicting subsets.

Data: the set $\mathcal{C}$ of the canonical decomposition.
Result: the set $\mathcal{S}_\Gamma$ of conflicting subsets.
Compute a partition $\{\mathcal{C}_1, \ldots, \mathcal{C}_M\}$ of $\mathcal{C}$, for instance using Algorithm 2;
Compute the indicator vector V of size $d = \prod_{j=1}^{M}(|\mathcal{C}_j| + 1)$ of the M-tuples of $\mathcal{C}$ that contain no consonant elements, for instance using Algorithm 3;
Initializations: $\mathcal{S}_\Gamma = \emptyset$;
for $n = 1 \ldots d$ **do**
  if the n th element of V is equal to 1 **then**
    Initializations: $\Gamma_{\emptyset_l} = \emptyset$; $B = \Omega$;
    for $j = 1 \ldots M$ **do**
      $i \leftarrow$ index of the element of $\mathcal{C}_j$ belonging to the M-tuple n;
      if $i > 0$ **then**
        $A \leftarrow$ the element of index i in $\mathcal{C}_j$;
        $\Gamma_{\emptyset_l} \leftarrow \Gamma_{\emptyset_l} \cup \{A\}$;
        $B \leftarrow B \cap A$;
      end
    end
    if $B = \emptyset$ **then**
      $\mathcal{S}_\Gamma \leftarrow \mathcal{S}_\Gamma \cup \{\Gamma_{\emptyset_l}\}$
    end
  end
end

Algorithm 2: Partition of $\mathcal{C}$ into consonant subsets.

Data: the set $\mathcal{C}$ of the canonical decomposition.
Result: the elements of a partition of $\mathcal{C}^*$ into consonant subsets.
Initializations: $\mathcal{C}' = \mathcal{C}^*$; $M = 0$;
while $\mathcal{C}' \neq \emptyset$ **do**
  $M \leftarrow M + 1$;
  $A \leftarrow$ an element of $\mathcal{C}'$ of minimal cardinality;
  $\mathcal{C}_M \leftarrow A$;
  $\mathcal{C}' \leftarrow \mathcal{C}' \backslash A$;
  while $\exists B \in \mathcal{C}' \mid \forall A \in \mathcal{C}_M, B \subseteq A$ *or* $A \subseteq B$ **do**
    $\mathcal{C}_M \leftarrow \mathcal{C}_M \cup \{B\}$;
    $\mathcal{C}' \leftarrow \mathcal{C}' \backslash B$;
  end
end

of the algorithm considers any pair of elements in two different consonant subsets, and if there is an inclusion relationship between them, then, for every M-tuple including this pair of elements, the value of the corresponding V component is set to 0.

Let us illustrate these algorithms on the previous example, with $\mathcal{C} = \{A_1, \ldots, A_6\}$. During the iterations of Algorithm 2, we have successively: $M = 1$, $\mathcal{C}_1 = \{A_1\}$, $\mathcal{C}_1 = \{A_1, A_2\}$, $\mathcal{C}_1 = \{A_1, A_2, A_5\}$, $M = 2$, $\mathcal{C}_2 = \{A_3\}$, $\mathcal{C}_2 = \{A_3, A_4\}$, $M = 3$, $\mathcal{C}_3 = \{A_6\}$. In this example, the elements of $\mathcal{C}$ are here scanned according to their binary representation order (where H_i is represented by a bit equal to 1 at the i^{th} position from the left). However, more optimized scans could be used in Algorithm 2 "while" loops. In Algorithm 3, V is of size $4 \times 3 \times 2 = 24$. First, the V values corresponding to 1-tuples are set to 0. Then, $V(0) = V(1) = V(2) = V(3) = V(4) = V(8) = V(12) = 0$. Then searching the inclusion relationships between elements in two different $\mathcal{C}_j$, $j \in \{1, 2, 3\}$, only one is found, namely $\{A_3\} \subset \{A_6\}$, i.e. between the 1^{st} element of $\mathcal{C}_2$ and the 1^{st} element of $\mathcal{C}_3$. Then, $V(16) = V(17) = V(18) = V(19) = 0$. Then, 13 potential conflicting subsets remain, namely $\{H_1, H_2\}$, $\{\{H_1, H_3\}, H_2\}$, $\{\{H_1, H_3, H_4\}, H_2\}$, $\{H_1, \{H_2, H_4, H_5\}\}$, $\{\{H_1, H_3\}, \{H_2, H_4, H_5\}\}$, $\{\{H_1, H_3, H_4\}, \{H_2, H_4, H_5\}\}$, $\{H_1, \{H_2, H_6\}\}$, $\{\{H_1, H_3\}, \{H_2, H_6\}\}$, $\{\{H_1, H_3, H_4\}, \{H_2, H_6\}\}$, $\{\{H_2, H_4, H_5\}, \{H_2, H_6\}\}$, $\{H_1, \{H_2, H_4, H_5\}, \{H_2, H_6\}\}$, $\{\{H_1, H_3\}, \{H_2, H_4, H_5\}, \{H_2, H_6\}\}$, $\{\{H_1, H_3, H_4\}, \{H_2, H_4, H_5\}, \{H_2, H_6\}\}$. Considering in addition the criterion of empty intersection (Algorithm 1), $\{\{H_1, H_3, H_4\}, \{H_2, H_4, H_5\}\}$ is found not satisfying it, so that finally $|\mathcal{S}_\Gamma| = 12$. Note that a brute-force algorithm, not using the notion of consonant subsets, would have to check Definition 1 for $2^{|\mathcal{C}|} - 1 - |\mathcal{C}|$, i.e. 57 cases in the example.

For further results using consonant subsets $\mathcal{C}_j$, one can refer to [39] (Roquel's PhD thesis), which also gives a formulation from the functions resulting from the combination of the conjunctive GSSF associated with the elements of a given $\mathcal{C}_j$.

Some numerical simulations have been performed to compare the proposed approach (using consonant subsets) to a brute-force approach that derives $\mathcal{S}_\Gamma$ by checking the full number of tuples. The computation time improvement depends on the number of consonant subsets that can be defined from the canonical decomposition of the considered BBA. For tests performed considering 10 000 SBBA random samples, the ratio between the average computation times of the brute force approach and the proposed one is about 20 for $|\mathcal{C}| = 3|\Omega|$, $|\Omega| \in \{6, \ldots, 10\}$, and can reach 100 for $|\mathcal{C}| = 24$, $|\Omega| = 4$.

Algorithm 3: Indicator vector of non-consonant M-tuples.

Data: the elements of a partition of $\mathcal{C}$ into consonant subsets.
Result: indicator vector V of the M-tuples of $\mathcal{C}$ that contain no consonant elements.
Initializations: $d \leftarrow \prod_{j=1}^{M}(|\mathcal{C}_j|+1)$; V is a boolean vector of size d initialized with the value 1 for each element; $s_1 = 1$;
for $j = 2 \dots M$ **do**
  $s_j \leftarrow s_{j-1}(|\mathcal{C}_{j-1}|+1)$;
end
for $j = 1 \dots M$ **do**
  for $i = 0 \dots |\mathcal{C}_j|$ **do**
    $V(s_j \times i) = 0$;
  end
end
for $i = 1 \dots M-1$ **do**
  forall the $A \in \mathcal{C}_i$ **do**
    $k \leftarrow$ the index of A in $\mathcal{C}_i$;
    for $j = i+1, M$ **do**
      forall the $B \in \mathcal{C}_j$ **do**
        $l \leftarrow$ the index of B in $\mathcal{C}_j$;
        if $A \subset B$ *or* $B \subset A$ **then**
          $p \leftarrow ks_i$;
          while $p < d$ **do**
            for $n = p, p + s_i - 1$ **do**
              if $V(n) = 1$ *and* $\frac{n}{s_j} \pmod{|\mathcal{C}_j|+1} = l$ **then**
                $V(n) = 0$;
              end
            end
            $p \leftarrow p + (|\mathcal{C}_i|+1)s_i$;
          end
        end
      end
    end
  end
end

Table 1
Correlation between $m(\emptyset)$ and $\overline{f_\emptyset}$ maximum value.

$\lvert\mathcal{C}\rvert$	2	3	4	5	6	7	8	9	10	11	12
R^2	1	0.989	0.967	0.936	0.875	0.796	0.697	0.578	0.443	0.332	0.332

4.2. Numerical tests

In this section, we propose numerical tests to investigate the potential correlation between $m(\emptyset)$ and some element(s) of the decomposition.

For this, random BBAs are uniformly drawn as in [7]. For $|\Omega| = 4$, for each BBA sample, the number of focal elements of the BBA is drawn uniformly in the interval $[2, 15]$, as their indices are drawn uniformly in the interval $[1, 2^\Omega - 1]$. Ω is always focal in order to ensure that the BBA is non-dogmatic. Then, for each focal element, a mass value is drawn according to the Gamma distribution giving an unnormalized mass function which is then normalized so that its sum equals 1. Note that the decomposition applies also when $m(\emptyset) = 0$. In this case, either m is an SBBA and all the terms of $\overline{f_\emptyset}$ are null, or m is not an SBBA and some terms of $\overline{f_\emptyset}$ are positive and some are negative. Let $\delta = m(\emptyset) - \sum_{A \in 2^\Omega} \overline{f_\emptyset}(A)$, where $\overline{f_\emptyset}$ is computed using Eq. (12). The mathematical proof shows that this quantity is theoretically equal to 0. However, the proposed numerical validation is intended to check the absence of numerical problems and we obtained the following statistics on δ values, computed from 11 300 BBA samples: mean value $= 6.8182 \times 10^{-11}$, L_1 norm $= 1.4002 \times 10^{-10}$ (average of the $|\delta|$ values), L_∞ norm $= 1.1325 \times 10^{-6}$ (maximum of the $|\delta|$ values).

In the previous simulations, we considered the general case of random BBAs. Now, in most practical cases, Dempster's conflict comes from the conjunctive combination of several BBAs. We now test the correlation between $m(\emptyset)$ and $\overline{f_\emptyset}$ terms in the case of an SBBA (that is by definition the conjunctive combination of SSFs). Table 1 shows the correlation (computed on 10 000 samples and versus $|\mathcal{C}|$) between $m(\emptyset)$ and the maximum value of the $\overline{f_\emptyset}$ terms, because the maximal value of the correlation is expected for this maximum value of the decomposition terms (since the BBA sample is an SBBA, the terms of the decomposition are all positive and sum up to $m(\emptyset)$). It clearly appears that if the correlation is high for small numbers of combined SSFs, when $|\mathcal{C}|$ increases the correlation decreases, reflecting the fact that several hypotheses contribute to $m(\emptyset)$.

Secondly, let us observe the distribution of $\overline{f_\emptyset}(A)$ versus $|A|$, by varying $|\Omega|$. For this simulation, only the separable case is considered so that $\forall A$, $\overline{f_\emptyset}(A) \geqslant 0$ and average values of $\overline{f_\emptyset}(A)$ can be compared easily. As previously, we use the uniform random sampling proposed in [7], but only SBBAs are retained (acceptance–rejection method). Table 2 shows the mean

Table 2
Mean value and standard deviation between parentheses of $\overline{f_{\emptyset}}(A)$ versus $|A|$, for different values of $|\Omega|$. Only separable BBAs are considered. N_s is the number of samples.

$\lvert A\rvert$	0	1	2	3	4	5
$\lvert\Omega\rvert = 2$	184×10^{-3}	145×10^{-5}	0.0			
$N_s = 8397$	(263×10^{-3})	(124×10^{-4})	(0.0)			
$\lvert\Omega\rvert = 3$	128×10^{-3}	387×10^{-5}	956×10^{-6}	0.0		
$N_s = 3975$	(206×10^{-3})	(178×10^{-4})	(841×10^{-5})	(0.0)		
$\lvert\Omega\rvert = 4$	695×10^{-4}	974×10^{-6}	219×10^{-6}	644×10^{-7}	0.0	
$N_s = 930$	(162×10^{-3})	(718×10^{-5})	(287×10^{-5})	(163×10^{-5})	(0.0)	
$\lvert\Omega\rvert = 5$	315×10^{-4}	881×10^{-7}	382×10^{-7}	573×10^{-8}	133×10^{-9}	0.0
$N_s = 558$	(122×10^{-3})	(264×10^{-5})	(186×10^{-5})	(320×10^{-6})	700×10^{-8}	(0.0)

value (and standard deviation) of $\overline{f_{\emptyset}}(A)$ versus $|A|$, for different values of $|\Omega|$. We clearly see that highest "local conflict function" values $\overline{f_{\emptyset}}(A)$ are achieved for the hypotheses with low cardinality, in particular the singleton hypotheses. We also note that when $|\Omega|$ increases, the conflict $m(\emptyset)$ is spread over more hypotheses leading to globally smaller values of $\overline{f_{\emptyset}}(A)$.

4.3. Toy example

We now propose a direct interpretation on a toy example illustrating the proposed decomposition. Let us consider a classification problem with c classes and two sources of observations. The aim of the classification is to estimate the class of a sample based on observations. Observations occur in a feature space. In the case of supervised classification, we assume that the link between this feature space and the class space is known. For instance, using probabilistic models, this link can be expressed through the conditional probability laws of an observation (features) conditionally to each class. Also classically, the feature space is assumed to be continuous and the observations are corrupted by a Gaussian white noise $\mathcal{N}(0, \sigma)$. Here, we assume that we have two sources providing two observations corrupted by an independent Gaussian noise, and we also assume that the conditional probability parameters, i.e. mean and standard deviation values, and thus the conditional probabilities of an observation conditionally to each class, are known.

Using the belief function framework, we consider the frame of discernment $\Omega = \{H_1, \ldots, H_c\}$, where H_i, $i \in \{1, \ldots, c\}$, corresponds to the hypothesis that the sample belongs to class i. For each observation in the feature space, a BBA is constructed, with the class set as discernment frame, to reflect the belief deduced from this observation about the possible class(es) corresponding to this observation. Then the BBAs derived from the different observations (two in our case) will be combined so that the decision is taken based on the combined BBA. The BBA allocation is performed according to the method proposed by Dubois and Prade [12], and based on the assumed equality between pignistic probabilities and conditional probabilities (in our case). In short this allocation is as follows: let us assume that $P(H_{j(1)}) \geqslant P(H_{j(2)}) \geqslant \cdots \geqslant P(H_{j(c)})$, the BBA has at most c focal elements among $\{H_{j(1)}\}, \{H_{j(1)}, H_{j(2)}\}, \ldots, \Omega \setminus \{H_{j(c)}\}$, and Ω, having masses respectively equal to $P(H_{j(1)}) - P(H_{j(2)})$, $2(P(H_{j(2)}) - P(H_{j(3)}))$, $(c-1)(P(H_{j(c-1)}) - P(H_{j(c)}))$, $cP(H_{j(c)})$. The constructed BBA is consonant.

Classically, the BBAs derived from the two sources would be combined, and a decision would be taken according to the combined BBA (e.g. in favor of the hypothesis maximizing the pignistic probability). In our case, we aim at analyzing the effects of a modeling error, in particular if it is visible on the $\overline{f_{\emptyset}}$ function. The considered error in this toy example is an overestimation of the *assumed* standard deviation of one class, namely H_2 (the *assumed* class parameters are used for the computation of the probabilities of the classes and then BBAs). So, the erroneous BBA will present a bias in favor of H_2. Our aim is to check if it induces a specific "local conflict function" value $\overline{f_{\emptyset}}(H_2)$.

The simulation is performed as follows. For each sample (in the presented results, the number of samples is 5000):

(i) a class i is drawn uniformly in $\{1, 2, \ldots, c\}$;
(ii) two observations are drawn according to the *actual* source conditional distributions of class i;
(iii) *assuming* normal class distributions with *parameters* (μ_j, σ_j), $j \in \{1, \ldots, c\}$, the two BBAs are built following the Dubois–Prade mass allocation [12];
(iv) BBAs are combined using the conjunctive rule (since sources are independent) and the proposed decomposition of the conflict is applied to the resulting BBA.

As previously said, we arbitrarily introduce an error (or imprecision) in the fusion model. Precisely this error deals with the *assumed* parameters of the conditional distribution used during step (iii) to construct the BBAs, that may differ from the *actual* parameters of the conditional distribution used during step (ii) to randomly draw the observations. In Fig. 1, $\Omega = \{H_1, H_2, H_3, H_4\}$, and the error on the model is related to the assumed standard deviation of class H_2 ($\sigma_i = \widetilde{\sigma}$). Fig. 1 shows that the value of $\overline{f_{\emptyset}}(H_2)$ is greater than for the other hypotheses, even if it is high for all singleton hypotheses: firstly because they may be in conflict with H_2 and secondly since singleton hypotheses present higher values of "local conflict" than other hypotheses as was observed in Table 2.

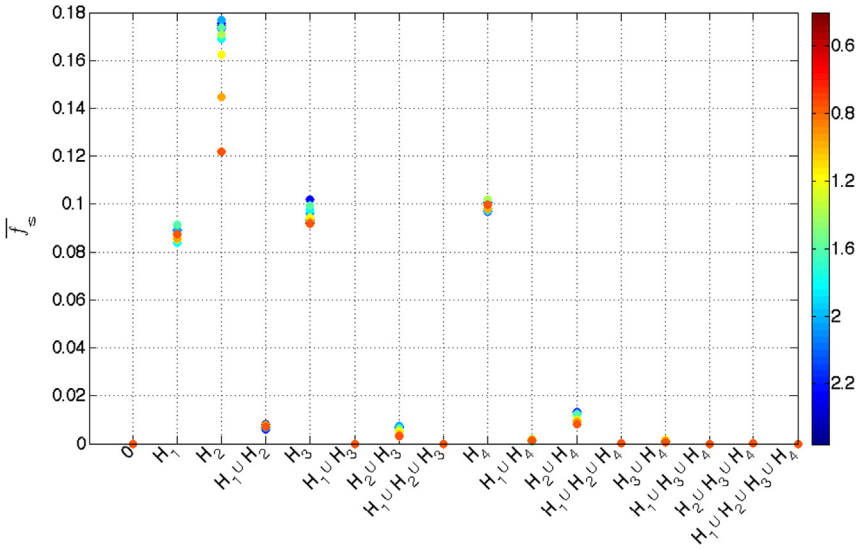

Fig. 1. $\overline{f_\emptyset}(A)$ versus hypothesis $A \in \{\emptyset, H_1, H_2, \{H_1, H_2\}, H_3, \{H_1, H_3\}, \{H_2, H_3\}, \{H_1, H_2, H_3\}, H_4, \{H_1, H_4\}, \{H_2, H_4\}, \{H_1, H_2, H_4\}, \{H_3, H_4\}, \{H_1, H_3, H_4\}, \{H_2, H_3, H_4\}, \Omega\}$. Toy example: for hypothesis H_2, the assumed value $\widetilde{\sigma}(\in [0.5, 2])$ is greater than its correct value ($\sigma = 0.5$, class center distance is 1). The largest $\overline{f_\emptyset}(A)$ value is obtained for $A = H_2$, i.e. the hypothesis which is poorly modeled, and which thus induces conflict.

This illustrates that the proposed decomposition helps identifying the potential source of the conflict among hypotheses.

5. Application to a localization problem

In this section, we illustrate the use of the conflict between sources as a diagnosis tool within a real system, namely a small autonomous robot. We use the proposed function of conflict in the problem of vehicle localization using several sources. For this application, we will assume that the conflict is a strong indicator of fusion correctness, i.e. when the conflict is important, the results of the fusion process may be questionable. In particular, we compare the results of the fusion either not taking into account any indicator of validity of the fusion (i.e. fusion is always assumed valid), or taking into account one of the two possible indicators of validity of the fusion, namely Dempster's conflict, and the conflict local to the favorite hypothesis of the fusion. This latter case uses our decomposition. The basic assumption is that the fusion remains correct when the conflict (when present) is brought by the other hypotheses than the one that would be chosen, whereas it is all the more questionable that the conflict is focused on the favorite assumption or on $\emptyset$. In our case we will use consonant BBAs, so that $\overline{f_\emptyset}(\emptyset)$ is null, and thus the conflict is actually focused on singletons of Ω or compound hypotheses.

5.1. Localization problem

Localization is a key problem in making truly autonomous robots (see e.g. [46] or [6] for a review). Indeed, either considering exploration robots or service/health-care robots to cite only two examples, the robot should generally move in its environment to accomplish its task. In order to achieve its objective, it should localize itself with respect to its environment using sensors which provide information about the environment around or about its own movements.

Classically, the robot embeds some odometers which are used to estimate the distance traveled by each wheel independently. Assuming a rigid structure of the robot, and knowing the diameter of the wheel and the axle spread, the displacement (longitudinal and rotational components) between two time instants is estimated and the robot localization is computed by integrating these data. The odometers are mainly reliable over short distances since wheel slippage can bias the acquired data. Moreover, due to the data integration, the localization errors accumulate over time.

In the last decade, the visual odometry was proposed [33]. It consists in using image data (instead of odometer data) to evaluate the robot displacement. Generally some key-points (e.g. SURF [3] or SIFT [23] points) are tracked in successive images to infer both the scene structure (3D) and the camera movement [2]. Thus, unlike odometers, visual odometry uses the environment surrounding the robot to estimate its localization. Then it is not affected by a wheel slipping, but it is limited by the image processing performance versus the robot environment (e.g. the key-point detection and matching). The absolute localization being computed by integration of displacements, error accumulation still occurs.

For exploration applications, the environment is unknown and the robot has to reconstruct the map of the environment while localizing itself into it. This is known as the SLAM (Simultaneous Localization And Mapping) problem [13,50]. SLAM algorithms estimate a state vector containing both the robot pose and the landmark locations. The robot pose information is usually expressed in the global frame while proprioceptive data are given in the robot local frame. Most of the proposed

methods [31] use both exteroceptive sensors (like laser range-finder or camera) to gather information about the environment and proprioceptive sensors (like odometers) to localize the robot. Classically, SLAM is done using probabilistic filters (e.g. Kalman filter [51], particle filter [31]). The data fusion process is composed of two steps. First, it uses proprioceptive sensors to compute the predicted state and then it corrects this state using exteroceptive sensors. Two directions are investigated in current works on localization problems: the instrumentation and embeddability of the systems, and the application of theoretical advances in filtering, such as the extensions of Kalman's filter (e.g. [36,4]). Recently, two methods for localization have been proposed based on interval analysis or on belief function theory [1,32]. The interval analysis is a rather widely used approach for localization problem (e.g. [15]). In [32], it is shown that it boils down to use categorical belief functions in the belief function framework. In [1], belief functions are used to define an algorithm to match a map (mainly road segments) considering also GPS data. In both studies, the conflict is not considered.

In the next section, we specify the data used as input of the fusion in our experiments.

5.2. Data

The *Rawseeds* project[3] aims at building benchmarking tools for robotic systems and evaluating the performances of these systems [5,8]. The project provides the ground truth corresponding to different trajectories followed by a robot, and the sensor data, either as raw data or processed by some algorithms.

In this study, we propose to combine the outputs of different localization algorithms in order to improve the localization precision. Three kinds of algorithms have been considered which provide the corresponding sources for the fusion. The first one (S_1) exploits only odometer data. The second one (S_2) exploits only images [34]. For both S_1 and S_2, data are provided by the *Rawseeds* database. Finally, the third algorithm (S_3), FastSlam algorithm [30], exploits both odometers and camera. For the three algorithms the estimated variables are the longitudinal and rotational components of displacement. These estimates are more or less precise depending on the physical world and the movement of the vehicle. A wheel sliding may induce an error in the estimates of the algorithms using odometer data; a homogeneous environment or a mismatch between features may induce an error for the algorithms using camera data.

5.3. Fusion model

In this section, we propose a simple way to model the problem and the data, with the primary objective to illustrate the interest of the proposed decomposition. Other models could be used as well. At each instant the movement is described by a couple $(\delta_s, \delta_\theta)$ (longitudinal and rotational components), whose values are bounded by the motor vehicle features. $(\delta_s, \delta_\theta)$ are expressed in the local robot frame. These values are not affected by the movement integration and do not depend on the robot pose. In this work, the δ_s and the δ_θ ranges have been discretized in a finite number of values, so that δ_s varies in $[0, 0.3\text{ m}]$ with a step equal to 6×10^{-3} m, and δ_θ varies in $[-0.2, 0.2]$ with a step equal to $\frac{1}{150}$ rad.

The frame of discernment Ω is the set of discrete pairs of values $(\delta_s, \delta_\theta)$, so that, according to the discretization, $|\Omega| = 50 \times 60$. $\overrightarrow{\delta_t^i} = (\delta_s^i(t), \delta_\theta^i(t))'$ denotes the measurement provided by a source i at instant t, and $\overrightarrow{\delta_H} = (\delta_s(H), \delta_\theta(H))'$ denotes the components associated with a hypothesis H. As a first assumption, we assume that, knowing the source estimate $\overrightarrow{\delta_t^i}$, the pignistic probability of a hypothesis H, $H \in \Omega$, can be calculated from a bidimensional Gaussian law centered around the observation values:

$$BetP(H) = \frac{1}{2\pi\sigma^2} \exp\left\{ \frac{-1}{2\sigma^2} \left(\left(\delta_s(H) - \delta_s(t)\right)^2 + \left(\delta_\theta(H) - \delta_\theta(t)\right)^2 \right) \right\}, \tag{19}$$

where σ is the standard deviation of the assumed Gaussian white noise. In our experiments, σ was assumed stationary over time and equal for the three considered sources. The higher the distance between hypothesis H and source estimates at t, the lower the probability of H.

Finally, a consonant BBA centered on the hypothesis maximizing Eq. (19) is provided by the mass allocation proposed in [12]. Indeed, as stated in Corollary 2, for such a BBA the $\overline{f_\emptyset}$ terms are null. Thus when analyzing $\overline{f_\emptyset}$ after combination, a non-null value can only come from a conflict between the sources that have been combined. For consonant BBAs, the number of focal elements is at most $|\Omega|$, but here for practical implementation, we restricted to 4 focal elements.

As second main hypothesis about the data model, we assume that the sampling of data (30 Hz) is high relatively to the acceleration so that $\delta_s^i(t)$ and $\delta_\theta^i(t)$ vary slowly over time. This is called "regularity assumption". This hypothesis allows us to consider the move estimates at time $(t-1)$ as an information source for the estimation of the correctness of the estimates at time t, or even as estimates of the move at t. We will see in the next subsection how the information at time $(t-1)$ is used in the fusion process.

Finally, for combination, independence between sources can only be assumed for S_1 and S_2, since S_1 and S_3 both use the odometer data, and that S_2 and S_3 both use the camera data. Therefore we use Smets' conjunctive combination for S_1 and S_2, and the cautious combination [10] for the other source pairs.

[3] http://www.rawseeds.org/.

5.4. Exploitation of conflict

In this work, we estimate dynamically the degree of correctness of the sources to improve the fusion robustness. The global conflict $m(\emptyset)$ is decomposed according to Eq. (18). In this application, we focus on one specific element of the decomposition, namely the $\overline{f_\emptyset}$ value associated with the hypothesis candidate to be chosen by the fusion. If this latter is conflictual (i.e. its $\overline{f_\emptyset}$ value is non-null), we assume that one source has provided an erroneous piece of information, and we search it in order to remove it from the combination. Rather than a majority criterion to decide the correct pieces of information, we prefer to base the correctness estimation on the regularity assumption, based on the local distance between measurements at successive instants. It allows us to focus on the information concerning the hypotheses of interest (the ones selected by the sources). For this we introduce the following local, i.e. given a pair of hypotheses, pseudo-distance between BBAs:

$$Dist_{A,B}(Pl_1, Pl_2) = \frac{1}{2}\left|\left(Pl_1(A) - Pl_2(A)\right) + \left(Pl_2(B) - Pl_1(B)\right)\right|, \tag{20}$$

where Pl_j, is the plausibility function associated with m_j, $j \in \{1,2\}$, and A and B denote two hypotheses of 2^Ω. Eq. (20) defines a pseudo-metric for any (A,B): it is non-negative and symmetrical by construction, for each Pl, $Dist_{A,B}(Pl, Pl) = 0$, and it satisfies the triangular inequality: $Dist_{A,B}(Pl_1, Pl_2) + Dist_{A,B}(Pl_2, Pl_3) \geqslant Dist_{A,B}(Pl_1, Pl_3)$.

The main interest of this local distance is to restrict to a subset of 2^Ω (pairs of elements) because our interest focuses on some hypotheses (typically those that can be selected when making the decision).

Precisely, if we denote by H_j and $H_{\textcircled{\scriptsize}}$ the singleton elements maximizing the plausibility function of respectively m_j and $m_{\textcircled{\scriptsize}}$, where m_j is the consonant BBA associated with source S_j described in Section 5.3 and $m_{\textcircled{\scriptsize}}$ is the BBA after combination of these BBAs, the exploitation of the conflict is composed of five steps:

1. Compute the set $\mathcal{C}$ of hypotheses of the canonical decomposition of $m_{\textcircled{\scriptsize}}$, and the set $\mathcal{S}_\Gamma$ of conflicting subsets $\Gamma_{\emptyset_l}$ (Definition 1).
2. Compute the level of conflict introduced by the singleton element chosen by the decision step: $\overline{f_\emptyset}(H_{\textcircled{\scriptsize}}) = \sum_{\Gamma_{\emptyset_l} | H_{\textcircled{\scriptsize}} \in \Gamma_{\emptyset_l}} \frac{1}{|\Gamma_{\emptyset_l}|} f_\emptyset(\Gamma_{\emptyset_l})$, with $f_\emptyset$ defined by Eq. (6).
3. If $\overline{f_\emptyset}(H_{\textcircled{\scriptsize}}) > 0$, then search the sources which do not respect the assumption of regularity: $Dist_{H_j(t),H_j(t-1)}(Pl_{j,t}, Pl_{j,t-1}) > T_D$, with

$$Dist_{H_j(t),H_j(t-1)}(Pl_{j,t}, Pl_{j,t-1}) = \frac{1}{2}\left|\left(Pl_{j,t}\left(H_j(t)\right) - Pl_{j,t-1}\left(H_j(t)\right)\right) + \left(Pl_{j,t-1}\left(H_j(t-1)\right) - Pl_{j,t}\left(H_j(t-1)\right)\right)\right|,$$

   where j is the source index, t and $t-1$ two successive instants, and $Pl_{j,t}$ is the plausibility function of source j at time t. The threshold value T_D has been fixed experimentally to 0.5.
4. Combine the sources which have been found as likely correct using the two conditions, to obtain a BBA $\hat{m}_{\textcircled{\scriptsize}}$.
5. Decide $\hat{H}(t)$ according to the maximum of the pignistic probability associated to $\hat{m}_{\textcircled{\scriptsize}}$.

Thus, a source S_i will be removed from the fusion process if, on the one hand, the combination of all sources leads to some conflict (measured via $\overline{f_\emptyset}$, Eq. (6)), and on the other hand, S_i does not satisfy the regularity assumption (measured via $Dist_{H_j(t),H_j(t-1)}(Pl_{j,t}, Pl_{j,t-1})$, Eq. (20)). Note that our approach is different from [22] where the author proposed to detect the conflict via a couple of measures, namely the mass of the empty set and the norm L_∞ of the difference between pignistic probabilities extended to 2^Ω. The two main differences relatively to [22] are: firstly, our measures are derived from functions defined over 2^Ω and secondly, the first measure (specific point of $\overline{f_\emptyset}$) is used to detect the conflict, and the second one ($Dist_{H_j(t),H_j(t-1)}(Pl_{j,t}, Pl_{j,t-1})$) is used to identify the source of conflict (according to the regularity assumption).

5.5. Results

Using the *Rawseeds* data to test our fusion algorithm, we choose a trajectory including several difficulties or situations that may induce errors for the robot's sensors, like corridors with doors on their sides, walls with different depths, spaces of different shapes and dimensions, with tables and chairs. Besides, the soil is very smooth, with occasional small ridges at junctions between different floor sections.

In this section, we present the results obtained from different fusion algorithms:

- a fusion scheme not taking into account the conflict: BBAs allocation based on Eq. (19); computation of $m_{\textcircled{\scriptsize}}$ (Section 5.4), i.e. BBAs conjunctive combination either using Smets rule or cautious rule [10] depending on source independence; decision in favor of $H_{\textcircled{\scriptsize}}$ (Section 5.4), i.e. according to the maximum pignistic probability. It is called "classic fusion".
- the proposed fusion method taking into account the conflict based on our conflict decomposition, as described in the five steps in Section 5.4. It is called "$\overline{f_\emptyset}$ based fusion".

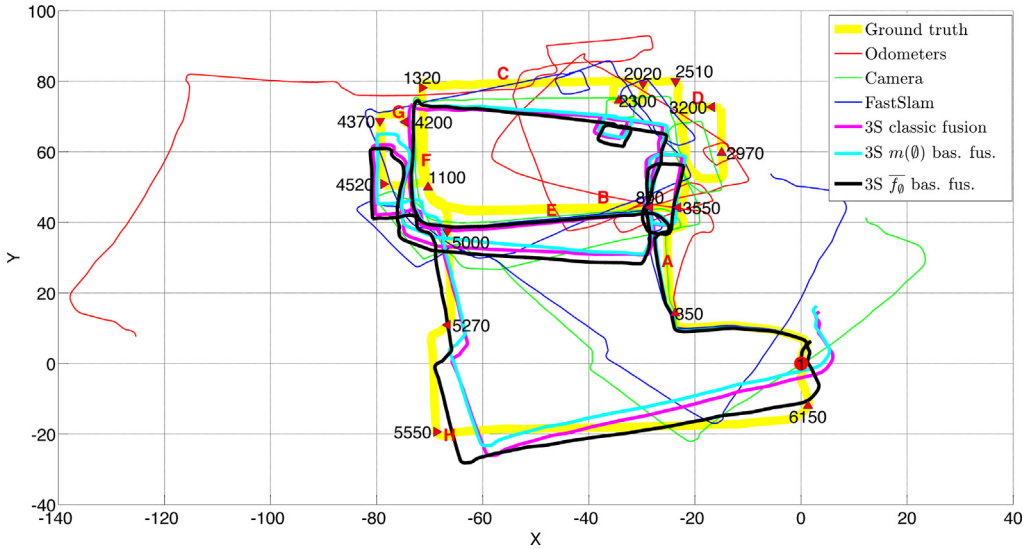

Fig. 2. *Rawseeds* trajectories. The integration of the movement estimation by odometer data (S_1), visual odometry (S_2) and FastSlam (S_3) algorithms are plotted in red, blue and green, respectively. The trajectory in black represents the integration of movement estimated by the proposed fusion method based on the interpretation of $\overline{f_\emptyset}$ values. For comparison, the trajectory resulting of the classical fusion of sources (i.e. not taking into account the conflict between sources) and the one resulting of a fusion depending on the $m(\emptyset)$ global conflict are shown in magenta and cyan, respectively. (For interpretation of the references to color in this figure legend, the reader is referred to the web version of this article.)

- an alternative fusion scheme taking into account the conflict based on $m(\emptyset)$: BBAs allocation and $m_{\textcircled{\emptyset}}$ computation; detection of conflict based on $m_{\textcircled{\emptyset}}(\emptyset)$ value; removing of the likely incorrect pieces of information (such that $Dist_{H_j(t),H_j(t-1)}(Pl_{j,t}, Pl_{j,t-1}) > T_D$) of the fusion as in the "$\overline{f_\emptyset}$ based fusion" scheme. It is called "$m(\emptyset)$ based fusion".

Most of the results will be expressed in terms of Root Mean Square Error (*RMSE*), defined as the root square of the L_2 norm, of three kinds of errors. The first one is the error on the basic estimates, namely δ_s and δ_θ. The second one is the error on the Cartesian coordinates of the displacement δ_x and δ_y. The third one is the error on the Cartesian coordinates of the location X and Y. These three representations are complementary since, on the one hand, the aim of localization is to obtain the best estimate of position in an absolute reference frame, and on the other hand, a "one-time" error may penalize the whole sequence of estimates in the absolute reference frame [20]. Considering δ_x and δ_y, the estimated values δ_θ are integrated (in contrary to the δ_s ones). It allows evaluating the estimation of the absolute angle θ that is a key parameter of displacement and localization.

As a global result and first guess of the performance, Fig. 2 presents a 2D top view of the 3D physical world with the ground truth trajectory and the different trajectories estimated by each individual source and different kinds of fusion. Qualitatively, we note that the mono-source estimations present a serious drift (the more imprecise being the odometer one). Conversely, we observe that the fusion prevents this drift effect. The figure also allows the qualitative comparison of three kinds of fusion: (i) classical evidential fusion according to the model presented in Section 5.3, (ii)–(iii) fusion only between likely correct sources when some conflict is detected, with source degree of correctness estimated on the basis of the regularity assumption as explained in Section 5.4. The conflict between sources can be detected either based on the proposed function $\overline{f_\emptyset}$, or based on $m(\emptyset)$ values. We observe that the conflict computed as described in Section 5.4 allows us to estimate a movement close to the ground truth even in extreme cases. We also observe that it outperforms the result of the fusion of the three sources not considering their degrees of correctness.

In order to further analyze the performance of the fusion, we performed some supplementary experiments. For comparison with the three source fusion scheme, we tested the combination of the two mainly complementary sources, namely S_1 (odometers) and S_2 (camera) versus the combination of the three sources (i.e. adding S_3, the FastSlam estimate). Quantitative analysis was based on Root Mean Square Error (*RMSE*). Results are summarized in Table 3.

Let us first analyze the performance for the variables directly estimated, namely $(\delta_s, \delta_\theta)$. From Table 3, we note that performances are very high, since the *RMSE* values are low, considering the precision of the map. Concerning the combination of two sources, we observe that the obtained results are within the interval of the mono-source performances. Comparing the different fusion results, for δ_s estimation, taking into account the conflict (either by "$m(\emptyset)$ based fusion" or by "$\overline{f_\emptyset}$ based fusion") improves the "classic" fusion results. Now, for two sources, the performances of the $m(\emptyset)$ based fusion and of the $\overline{f_\emptyset}$ based fusion are almost identical. Indeed we observe that, combining two consonant sources, the conflict, when it exists, is concentrated on a small number of hypotheses. When adding the third source, an improvement of the "classic" fusion results can be observed on both δ_s and δ_θ estimations. Finally for $(\delta_s, \delta_\theta)$, the difference of performances between classic

Table 3
Performance of localization from the 2D fusion model. Performance is measured in terms of $(\delta_s, \delta_\theta)$, (δ_x, δ_y) and (X, Y) *RMSE* estimations.

RMSE		$\delta_s \times 10^{-3}$	$\delta_\theta \times 10^{-3}$	$\delta_x \times 10^{-3}$	δ_y	X	Y
1 source	Odometers	0.526	0.219	88.1	80.9	38.3	36.1
	Camera	0.647	0.191	46.6	44.7	16.6	16.5
2 sources	Classic fusion	0.588	0.200	21.9	21.5	7.67	6.60
	$m(\emptyset)$ based fusion	0.539	0.200	19.8	19.5	6.77	6.81
	$\overline{f_\emptyset}$ based fusion	0.539	0.200	19.4	18.3	6.12	5.98
1 source	FastSlam	0.573	0.202	33.3	33.1	15.3	13.3
3 sources	Classic fusion	0.562	0.190	16.2	18.2	5.16	9.00
	$m(\emptyset)$ based fusion	0.549	0.189	16.3	18.0	4.80	10.0
	$\overline{f_\emptyset}$ based fusion	0.542	0.189	15.8	16.6	4.67	8.30

fusion and conflict based fusion is smaller for 3-source fusion than for 2-source fusion, mainly due to the performance of classical fusion.

Now the (δ_x, δ_y) values correspond to the estimated displacement expressed in the global frame. Unlike $(\delta_s, \delta_\theta)$, these estimates take into account the movement integration. Observing the results, the interest of the fusion is obvious (with a factor between 2 and 6 between monosource and multisource *RMSE* values). The variables (δ_x, δ_y) are estimated from δ_s and θ, that is the integral of the δ_θ values. Thus for (δ_x, δ_y) estimation performances, the rotational component estimation is by far the most sensitive parameter (explaining the very poor performance of the odometers). We note that, as a kind of fusion between odometer and camera data, the FastSlam algorithm also presents improved results relatively to the two other sources. We also note that taking into account the conflict also further reduces the *RMSE*, and finally that three source fusion provides even better results, especially when the conflict is considered, and when using $\overline{f_\emptyset}$ based local measure of conflict.

Finally, the performances for (X, Y), i.e. localization, are strongly related to those of (δ_x, δ_y), except for the *RMSE* of Y estimation in the three source fusion scheme. This worse result (relatively to the two source one) is due to a shift introduced (typically the case of a "one-time" error) at about a third of the course which biases all the following estimates of Y.

Let us now analyze the performances versus the location within the trajectory. Fig. 3 shows the *RMSE* values on δ_s, δ_θ, δ_x and δ_y estimations, respectively, considering either one source or two sources combined according to the different fusion processes. The plotted curves have been smoothed over 350 successive samples (sliding window). Fig. 3 confirms that the results obtained by fusion are much better than monosource results. In particular, we note the drift δ_x and δ_y due to accumulated errors in the case of the one-source estimates, whereas, in the case of the two-source estimates (either "classic" fusion or conflict based fusion), the *RMSE* remains about constant versus the time or indice sample (no observable drift). Now, comparing the different fusion schemes, the results of the fusion taking into account the conflict are better than those provided by the classical fusion. We also observe that generally δ_s estimation from odometer data is rather precise whereas δ_θ odometer estimation is rather poor (with a difference in RMSE values about 0.01 m), whereas δ_θ estimation from camera data is rather precise whereas δ_s camera estimation is rather poor (differences are about 0.003 rad). These differences in the estimation quality are partially due to the physical principle of the sensors themselves, and partially due to noise effects (and thus not systematic). Then, even if fusion results may be (slightly) worse than odometer ones for δ_s, they are much better on δ_θ, and vice versa for the comparison with the camera results. Since odometers provide the best estimate for δ_s (according to the *RMSE* criterion), and the camera provides the best estimate for δ_θ, one could think that the best way to combine the sources would be simply to use the odometers for longitudinal component, and the camera for the rotational one. We also tested this approach, called "ad-hoc" fusion in Fig. 3. The obtained results are very close to the camera results, mainly because of the predominant effect on the performance of the rotational component. However, globally the ad-hoc estimation is slightly better than the camera one, and sometimes quite better e.g. on δ_y around time sample 5000 ± 200. Indeed around this time, the camera δ_s estimation is very poor (conversely to the odometer one), and the robot moves approximately parallel to the Y-axis (see Fig. 2). Thus, even if the δ_s odometer estimation is statistically far better than the camera one, as the δ_θ camera estimation is statistically far better than the odometer one, the better combination of these two data is not to simply use odometer for longitudinal component, and the camera for the rotational one. Indeed, these two estimates should not be considered independently: for the odometers, a rotational component error corresponds to an error on the relative movement of the wheels, and thus also at least a slight error on the longitudinal component, and for the camera, a longitudinal component error may correspond to an error in the matching (of image features), and thus also an error on the rotational component. Moreover, since odometers as well as camera estimate the two components at once (not independently), the respective errors on the two components can compensate each other (the "best" estimate is the pair) conversely to what happens when considered independently.

Fig. 4 is similar to Fig. 3 but considering the three sources. We see that, for the estimation of δ_s, the fusion schemes based on conflict interpretation achieve almost the same performances as the odometers (red curve), and for the estimation of δ_θ, in most cases, the conflict based fusion schemes almost achieve the same performances as the camera data (blue curve). We note that now some differences appear between the $m(\emptyset)$ based fusion and the $\overline{f_\emptyset}$ based fusion, even if the results remain similar (indeed, this is the same process for selecting the likely correct sources, described in Section 5.4). For a more detailed

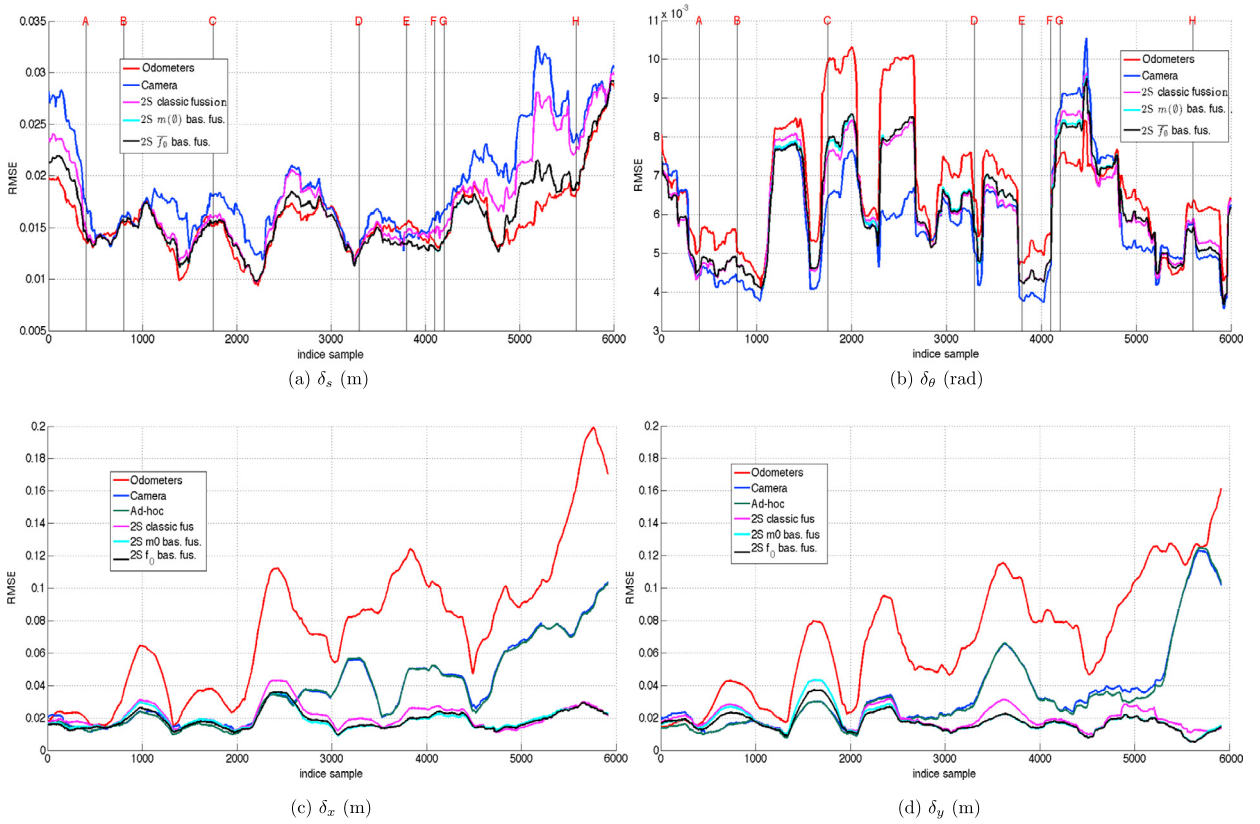

(a) δ_s (m) (b) δ_θ (rad)

(c) δ_x (m) (d) δ_y (m)

Fig. 3. *RMSE* values on (a) δ_s, (b) δ_θ, (c) δ_x, and (d) δ_y estimations by individual sources or by two-source fusion processes, using classical fusion or taking into account the conflict either via $m(\emptyset)$ or via $\overline{f_\emptyset}$.

understanding, Table 4 shows the percentages of each choice in terms of selected sources. Let us consider the four fusion methods with a variable set of sources (depending on the detected conflict and the criterion of regularity), namely $m(\emptyset)$ based fusion or $\overline{f_\emptyset}$ based fusion, either for 2 or 3 sources. For each one, Table 4 gives the percentage of selected sources among S_1 (Odometers), S_2 (Camera) and (S_1, S_2) for the two-source fusion methods, and among S_1, S_2, S_3 (FastSlam), (S_1, S_2), (S_1, S_3), (S_2, S_3) and (S_1, S_2, S_3) for the three-source fusion methods. For two-source fusion schemes, as already said, the two criteria for detecting a conflict (either based on $m(\emptyset)$ or $\overline{f_\emptyset}$) lead to very similar results, and we note that in more than 92% of cases both sources are taken into account. For the three-source fusion, the two criteria are not correlated (correlation coefficient equal to 0.528), and lead to different choices, in particular according to $\overline{f_\emptyset}$ the combination of the three sources should be less often chosen (89% against 98% of cases). Now a high value for the percentage of use of the whole set of sources, in conflict based fusion schemes, means that all information pieces provided by the different sources have been estimated as correct, either because they are effectively, or because the system is not able to detect that the fusion may be incorrect and to identify the wrong information piece.

In Figs. 3 and 4, several subparts of the trajectories have been identified (see Fig. 2): $[A, B]$ is a turn (at approximately $\frac{+\pi}{2}$: first $\frac{-\pi}{2}$ to the right and then $+\pi$), $[C, D]$ contains two successive loops (each one with four close turns at $\frac{\pm\pi}{2}$), $[E, F]$ is a straight line with a single turn at $\frac{-\pi}{2}$, $[G, H]$ contains a loop followed by successive turns at $\frac{\pm\pi}{2}$. From Figs. 3 and 4, we observe that most of the difficulties to estimate δ_θ occur in the case of successive close turns. For δ_s it is more difficult to identify the causes of errors, but we assume some wheel slippage.

As a conclusion of the whole study, we can say that in some cases, the knowledge of a more precise information than the global conflict can improve the results and the proposed method allows to identify this more precise information.

6. Conclusion

In this paper we introduced a "local conflict function" to compute the disagreement between sources. It is based on the decomposition of the mass of the empty set over subsets expressing the conflict. A strong point is the uniqueness of this decomposition. It relies on the interpretation of the GSSFs of the canonical decomposition as beliefs that might conflict. Thus, basically the proposed conflict decomposition applies for any given BBA and the analysis of its "internal" conflict. Practically, and because the notion of internal conflict remains ill-defined, we propose to apply the conflict decomposition to the result of the combination of "zero internal conflict" BBAs, namely consonant BBAs. In such a case, the proposed decomposition

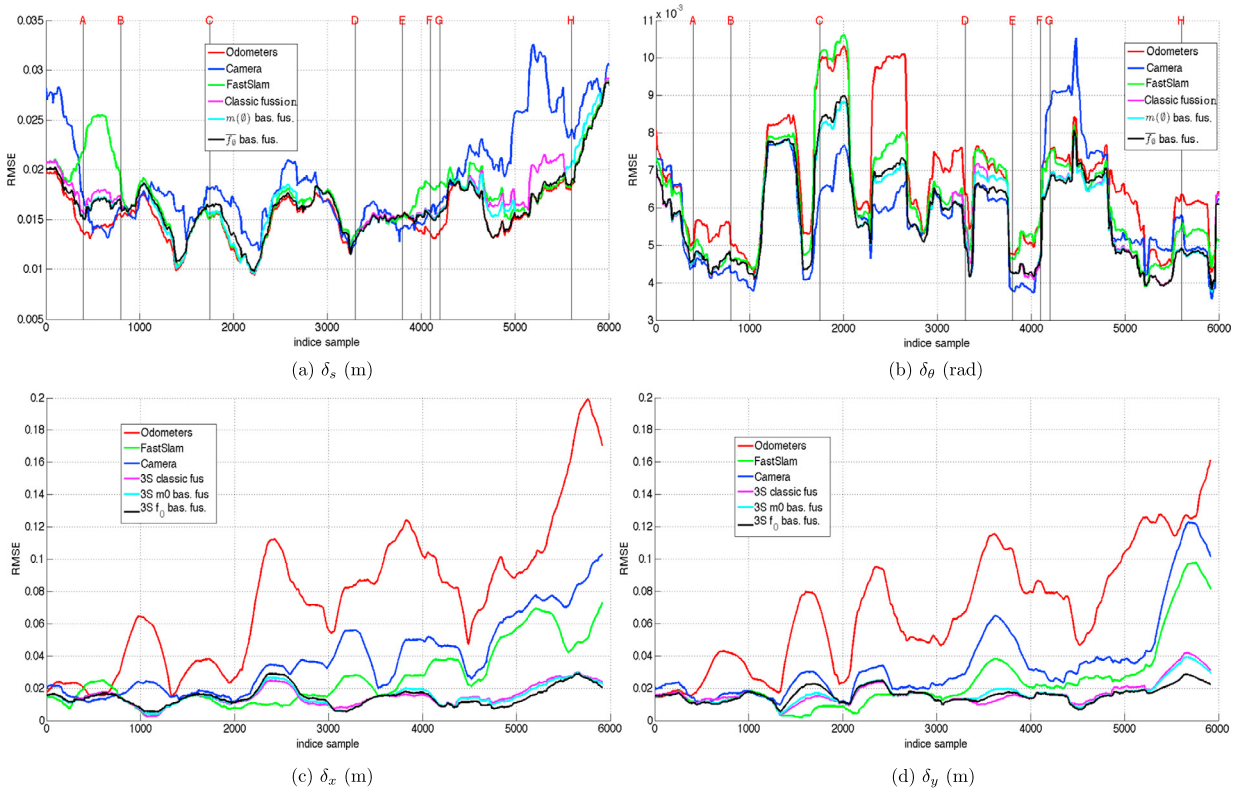

Fig. 4. *RMSE* values on (a) δ_s, (b) δ_θ, (c) δ_x and (d) δ_y estimations by individual sources or by three-source fusion processes, using classical fusion or fusion taking into account the conflict either via $m(\emptyset)$ or via $\overline{f_\emptyset}$. (For interpretation of the references to color in this figure, the reader is referred to the web version of this article.)

Table 4
Percentage of use of a given subset of sources, in conflict based fusion schemes.

	2 sources		3 sources	
Fusion based on	$m(\emptyset)$	$\overline{f_\emptyset}$	$m(\emptyset)$	$\overline{f_\emptyset}$
Odometers	5.6%	6.5%	0.05%	1.6%
Camera	0.9%	1.4%	0.03%	0.9%
FastSlam			0.02%	0.7%
Odom. and Camera	93.5%	92.1%	0.40%	2.7%
Odom. and FastSlam			1.10%	4.4%
Camera and FastSlam			0.00%	0.5%
3 sources			98.40%	89.2%

provides a tool to analyze *a posteriori* if there is some conflicting piece of information that could have corrupted the fusion result.

Theoretical and experimental examples have shown that a global measure such as Dempster's conflict or a dissimilarity measure does not always allow a fine analysis of source reliability and origin of the conflict, while the proposed local conflict function does.

Further analysis of the properties of the local conflict function, more experiments on other applications, and potential exploitation for model revision or conflict mass redistribution are planned for our future work. In particular, since, when combining two non-dogmatic BBAs, their elements of the canonical decomposition are mixed up, there is no way nowadays to distinguish the origin of the conflict between the conflict due to their (conjunctive) combination or the conflict already present in the individual BBAs. Now, the origin of the conflict could be simply preserved, if we label the elements of the canonical decomposition in terms of "original" BBA, and if we analyze the labels of the conflicting subsets. Future work could also address the complexity problems related to large discernment frames. A hint could be to develop stochastic approaches, such as Monte-Carlo methods, to approximate the computations.

Acknowledgements

This work was partially funded by a grant from DIGITEO (GESTCONFL project). The authors are grateful to the reviewers for their useful and detailed comments and suggestions, that helped a lot improving the paper.

References

[1] F. Abdallah, G. Nassreddine, T. Denœux, A multiple-hypotheses map matching method suitable for weighted and box-shaped state estimation for localization, IEEE Trans. Intell. Transp. Syst. 12 (4) (2011) 1495–1510.
[2] A. Bak, S. Bouchafa, D. Aubert, Detection of independently moving objects through stereo vision and ego-motion extraction, in: IEEE Intelligent Vehicles Symposium (IV), 2010, pp. 863–870.
[3] H. Bay, A. Ess, T. Tuytelaars, L. Van Gool, Speeded-up robust features (SURF), Comput. Vis. Image Underst. 110 (3) (2008) 346–359.
[4] A. Benavoli, B. Noack, Pushing Kalman's idea to the extremes, in: 15th International Conference on Information Fusion, IEEE, 2012, pp. 1202–1209.
[5] A. Bonarini, W. Burgard, G. Fontana, M. Matteucci, D.G. Sorrenti, J. Tardos, Rawseeds: Robotics advancement through web-publishing of sensorial and elaborated extensive data sets, in: Proceedings of IROS'06 Workshop on Benchmarks in Robotics Research, 2006.
[6] J. Borenstein, H.R. Everett, L. Feng, Navigating Mobile Robots: Systems and Techniques, A.K. Peters, Ltd., Wellesley, MA, 1996.
[7] T. Burger, S. Destercke, How to randomly generate mass functions, Int. J. Uncertain. Fuzziness Knowl.-Based Syst. 21 (5) (2013) 645–673.
[8] S. Ceriani, G. Fontana, A. Giusti, D. Marzorati, M. Matteucci, D. Migliore, D. Rizzi, D. Sorrenti, P. Taddei, Rawseeds ground truth collection systems for indoor self-localization and mapping, Auton. Robots 27 (4) (2009) 353–371.
[9] M. Daniel, Conflicts within and between belief functions, in: International Conference on Information Processing and Management of Uncertainty in Knowledge-Based Systems (IPMU), Dortmund (Germany), 2010, pp. 696–705.
[10] T. Denœux, Conjunctive and disjunctive combination of belief functions induced by nondistinct bodies of evidence, Artif. Intell. 172 (2–3) (2008) 234–264.
[11] S. Destercke, T. Burger, Toward an axiomatic definition of conflict between belief functions, IEEE Trans. Syst. Man Cybern., Part B 43 (2) (2013) 585–6596.
[12] D. Dubois, H. Prade, Representation and combination of uncertainty with belief functions and possibility measures, Comput. Intell. 4 (3) (1988) 244–264.
[13] A. Eudes, M. Lhuillier, S. Naudet-Collette, M. Dhome, Fast odometry integration in local bundle adjustment-based visual SLAM, in: International Conference on Pattern Recognition, Washington, DC, USA, 2010, pp. 290–293.
[14] M.C. Florea, A.-L. Jousselme, E. Bossé, D. Grenier, Robust combination rules for evidence theory, Inf. Fusion 10 (2) (2009) 183–197.
[15] A. Gning, P. Bonnifait, Constraints propagation techniques on intervals for a guaranteed localization using redundant data, Automatica 42 (7) (2006) 1167–1175.
[16] D. Harmanec, G.J. Klir, Measuring total uncertainty in Dempster–Shafer theory, Int. J. Gen. Syst. 22 (4) (1994) 405–419.
[17] V. Huynh, Y. Nakamori, Notes on "Reducing algorithm complexity for computing an aggregate uncertainty measure", IEEE Trans. Syst. Man Cybern., Part A, Syst. Hum. 40 (2010) 205–209.
[18] A.-L. Jousselme, P. Maupin, Distances in evidence theory: Comprehensive survey and generalizations, Int. J. Approx. Reason. 53 (2) (2012) 118–145.
[19] J. Klein, O. Colot, Singular sources mining using evidential conflict analysis, Int. J. Approx. Reason. 52 (9) (2011) 1433–1451.
[20] R. Kümmerle, B. Steder, C. Dornhege, M. Ruhnke, G. Grisetti, C. Stachniss, A. Kleiner, On measuring the accuracy of slam algorithms, Auton. Robots 27 (4) (2009) 387–407.
[21] E. Lefevre, O. Colot, P. Vannoorenberghe, Belief function combination and conflict management, Inf. Fusion 3 (2) (2002) 149–162.
[22] W. Liu, Analyzing the degree of conflict among belief functions, Artif. Intell. 170 (11) (2006) 909–924.
[23] D. Lowe, Distinctive image features from scale-invariant keypoints, Int. J. Comput. Vis. 60 (2) (2004) 91–110.
[24] Y. Maeda, H.T. Nguyen, H. Ichihashi, Maximum entropy algorithms for uncertainty measures, Int. J. Uncertain. Fuzziness Knowl.-Based Syst. 1 (1) (1993) 69–93.
[25] A. Martin, Reliability and combination rule in the theory of belief functions, in: International Conference on Information Fusion, Seattle (WA, USA), 2009, pp. 529–536.
[26] A. Martin, About conflict in the theory of belief functions, in: T. Denœux, M.-H. Masson (Eds.), Belief Functions: Theory and Applications: Proceedings of the 2nd International Conference on Belief Functions, Compiègne (France), 9–11 May, in: Advances in Intelligent and Soft Computing, vol. 164, 2012, pp. 161–168.
[27] A. Martin, A.-L. Jousselme, C. Osswald, Conflict measure for the discounting operation on belief functions, in: IEEE 11th Annual Conference on Information Fusion, Cologne (Germany), 2008, pp. 1003–1010.
[28] A. Martin, C. Osswald, Toward a combination rule to deal with partial conflict and specificity in belief functions theory, in: International Conference on Information Fusion, Québec (Canada), 2007, pp. 1–8.
[29] A. Meyerowitz, F. Richman, E. Walker, Calculating maximum-entropy probability for belief functions, Int. J. Uncertain. Fuzziness Knowl.-Based Syst. 2 (1994) 377–389.
[30] M. Montemerlo, S. Thrun, D. Koller, B. Wegbreit, FastSLAM: A factored solution to the simultaneous localization and mapping problem, in: AAAI National Conference on Artificial Intelligence, Menlo Park, CA, 2002, pp. 593–598.
[31] M. Montemerlo, S. Thrun, D. Koller, B. Wegbreit, FastSLAM 2.0: An improved particle filtering algorithm for simultaneous localization and mapping that provably converges, in: International Joint Conference on Artificial Intelligence, Acapulco, Mexico, 2003, pp. 1151–1156.
[32] G. Nassreddine, F. Abdallah, T. Denœux, State estimation using interval analysis and belief function theory: Application to dynamic vehicle localization, IEEE Trans. Syst. Man Cybern., Part B 40 (5) (2010) 1205–1218.
[33] D. Nister, O. Naroditsky, J.R. Bergen, Visual odometry, in: IEEE Computer Society Conference on Computer Vision and Pattern Recognition, Washington, DC, USA, 2004, pp. 652–659.
[34] P. Pinies, L.M. Paz, J.D. Tardós, CI-Graph: An efficient approach for large scale SLAM, in: International Conference on Robotics and Automation, 2009, pp. 3913–3920.
[35] E. Ramasso, C. Panagiotakis, M. Rombaut, D. Pellerin, Belief scheduler based on model failure detection in the TBM framework. Application to human activity recognition, Int. J. Approx. Reason. 51 (7) (2010) 846–865.
[36] B. Ristic, S. Arulampalm, N.J. Gordon, Beyond the Kalman Filter: Particle Filters for Tracking Applications, Artech House Publishers, 2004.
[37] C. Rominger, A. Martin, Using the conflict: An application to sonar image registration, in: Workshop on the Theory of Belief Functions, Brest (France), 2010, pp. 1–6.
[38] C. Rominger, A. Martin, A. Khenchaf, Laanaya, Sonar image registration based on conflict from belief function theory, in: International Conference on Information Fusion, Seattle (WA, USA), 2009, pp. 1317–1324.
[39] A. Roquel, Exploitation du conflit entre capteurs pour la gestion d'un système complexe multi-capteurs, PhD thesis, University Paris-Sud (France), 2012.

[40] A. Roquel, S. Le Hégarat-Mascle, I. Bloch, B. Vincke, A new local measure of disagreement between belief functions – application to localization, in: T. Denœux, M.-H. Masson (Eds.), Belief Functions: Theory and Applications: Proceedings of the 2nd International Conference on Belief Functions, Compiègne (France), 9–11 May, in: Advances in Intelligent and Soft Computing, vol. 164, 2012, pp. 335–342.
[41] J. Schubert, Clustering decomposed belief functions using generalized weights of conflict, Int. J. Approx. Reason. 48 (2) (2008) 466–480.
[42] J. Schubert, Conflict management in Dempster–Shafer theory using the degree of falsity, Int. J. Approx. Reason. 52 (3) (2011) 449–460.
[43] J. Schubert, Constructing and evaluating alternative frames of discernment, Int. J. Approx. Reason. 53 (2012) 176–189.
[44] J. Schubert, The internal conflict of a belief functions, in: T. Denœux, M.-H. Masson (Eds.), Belief Functions: Theory and Applications: Proceedings of the 2nd International Conference on Belief Functions, Compiègne (France), 9–11 May, in: Advances in Intelligent and Soft Computing, vol. 164, 2012, pp. 169–178.
[45] G. Shafer, A Mathematical Theory of Evidence, Princeton University Press, 1976.
[46] R. Simmons, R. Goodwin, K. Haigh, S. Koenig, J. O'Sullivan, A layered architecture for office delivery robots, in: The First International Conference on Autonomous Agents, ACM, Marina del Rey, CA, 1997, pp. 245–252.
[47] F. Smarandache, J. Dezert, Advances and Applications of DSmT for Information Fusion – Collected Works, American Research Press, Rehoboth, USA, 2006.
[48] P. Smets, The combination of evidence in the transferable belief model, IEEE Trans. Pattern Anal. Mach. Intell. 12 (5) (1990) 447–458.
[49] P. Smets, The canonical decomposition of a weighted belief, in: 14th International Joint Conference on Artificial Intelligence, Morgan Kaufmann Publishers Inc., San Francisco, CA, USA, 1995, pp. 1896–1901.
[50] S. Thrun, Learning metric-topological maps for indoor mobile robot navigation, Artif. Intell. 99 (1) (1998) 21–71.
[51] J.W. Weingarten, R. Siegwart, EKF-based 3D SLAM for structured environment reconstruction, in: IEEE/RSJ International Conference on Intelligent Robots and Systems, 2005, pp. 3829–3834.
[52] R.R. Yager, On the Dempster–Shafer framework and new combination rules, Inf. Sci. 41 (2) (1987) 93–137.